Plasma Physics Reports, Vol. 27, No. 9, 2001, pp. 813–818. Translated from Fizika Plazmy, Vol. 27, No. 9, 2001, pp. 859–864.

LOW-TEMPERATURE PLASMA

Investigation of the Electron Energy Distribution Function in Hollow-Cathode Glow Discharges in Nitrogen and Oxygen

V. Yu. Bazhenov, A. V. Ryabtsev, I. A. Soloshenko, A. G. Terent'eva, V. A. Khomich, V. V. Tsiolko, and A. I. Shchedrin

Institute of Physics, National Academy of Sciences of Ukraine, pr. Nauki 144, Kiev, 03039 Ukraine

Received February 15, 2001

Abstract—The mechanism for the formation of the inverse electron distribution function is proposed and realized experimentally in a nitrogen plasma of a hollow-cathode glow discharge. It is shown theoretically and experimentally that, for a broad range of the parameters of an N_2 discharge, it is possible to form a significant dip in the profile of the electron distribution function in the energy range $\varepsilon = 2$–4 eV and, accordingly, to produce the inverse distribution with $df(\varepsilon)/d\varepsilon > 0$. The formation of a dip is associated with both the vibrational excitation of N_2 molecules and the characteristic features of a hollow-cathode glow discharge. In such a discharge, the applied voltage drops preferentially across a narrow cathode sheath. In the main discharge region, the electric field E is weak ($E < 0.1$ V/cm at a pressure of about $p \sim 0.1$ torr) and does not heat the discharge plasma. The gas is ionized and the ionization-produced electrons are heated by a beam of fast electrons (with an energy of about 400 eV) emitted from the cathode. A high-energy electron beam plays an important role in the formation of a dip in the profile of the electron distribution function in the energy range in which the cross section for the vibrational excitation of nitrogen molecules is maximum. A plasma with an inverted electron distribution function can be used to create a population inversion in which more impurity molecules and atoms will exist in electronically excited states. © *2001 MAIK "Nauka/Interperiodica".*

1. INTRODUCTION

In recent years, numerous technological applications of low-pressure gas discharges in nitrogen and nitrogen-containing mixtures have stimulated active experimental and theoretical investigations of the electron energy distribution function (EEDF) in order to gain a better insight into the physics of the plasmochemical processes occurring in various plasma devices (see, e.g., [1–8]).

First of all, we should note that the shape of the EEDF is highly sensitive to the type of discharge and its parameters even in experiments with the same gas mixtures. Thus, in [1–4], the EEDF in N_2 and N_2–O_2 mixtures was studied under conditions such that the electric field was stronger than the breakdown field and was the only factor responsible for the heating of plasma electrons. In those papers, the EEDF $f(\varepsilon)$ was found to be monotonic ($df(\varepsilon)/d\varepsilon < 0$), but with different temperatures in different energy ranges. Such a shape of the EEDF is associated with the fact that, under those conditions, the distribution of the plasma electrons rapidly becomes Maxwellian under the action of the electric field.

On the contrary, in [5–8], it was shown that, in a weak electric field in the post-discharge plasmas of repetitive discharges in N_2 and Ar–N_2 mixtures, an important role in the formation of the EEDF is played by superelastic collisions, because, during the period between successive discharges, the electrons are heated only by energy transfer from vibrationally and electronically excited molecules to the plasma. As a result, the EEDF becomes peaked at energies that correlate with the excitation energies of the vibronic (vibrational–electronic) levels of molecules.

Our paper is devoted to an experimental and theoretical investigation of the EEDF in discharges that differ radically from both those studied in [1–4] and those studied in [5–8]. Specifically, we are interested in steady hollow-cathode glow discharges in nitrogen and oxygen. In such discharges, which are widely used in various technological applications, the applied voltage drops preferentially across a narrow cathode sheath. According to our measurements, the electric field E in the main discharge region was at most 0.1 V/cm (at a pressure of about $p \sim 0.1$ torr), which is one order of magnitude weaker than that in [1–4]. In our experiments, the gas was ionized and the plasma electrons were heated by a beam of fast electrons (with an energy of about 400 eV) emitted from the cathode. We show that, in such discharges in nitrogen, the formation of a significant dip in the EEDF in the energy range 2–4 eV and, accordingly, the inversion of the EEDF ($df(\varepsilon)/d\varepsilon > 0$) are attributed to the vibrational excitation of N_2 molecules. In contrast, in discharges in oxygen, the EEDF is monotonic because, on the one hand, it is cut off at low threshold energies for the excitation of the lowest lying electronically excited metastable states of O_2 molecules and, on the other hand, the cross sections for the excita-

1063-780X/01/2709-0813$21.00

tion of the vibrational levels of oxygen molecules are small.

2. EXPERIMENTAL SETUP AND MEASUREMENT RESULTS

The experiments were carried out with a hollow cylindrical cathode 280 mm in diameter and 400 mm in length. A 230-mm-diameter anode was placed near one end of the cathode. The vacuum chamber was pre-evacuated by a forepump to a residual pressure of 5×10^{-3} torr. Then, the chamber was filled with the working gas (nitrogen or oxygen) in the pressure range from 3×10^{-2} to 1×10^{-1} torr. The discharge current and applied voltage were varied in the ranges 0.5–0.9 A and 400–600 V, respectively. The plasma density, electric fields, and EEDF were measured by a pair of single Langmuir probes [9] made of tungsten wires 100 μm in diameter, the receiving sections being from 10 to 15 mm in length. The probes were designed so as to provide measurements along and across the symmetry axis of the cathode. In order for the measured current–voltage (*I–V*) characteristics of the probes to be immune to probe-surface contamination, the probes were cleaned after each measurement by heating them to a temperature of about 800° C with a dc source.

The EEDF was determined numerically by differentiating the *I–V* characteristics twice with (if necessary) preinterpolation of the measured data. The measurement accuracy was increased using the modified method described in [2], which is based on a specially devised programmable diagnostic system controlled by a personal computer. At each step of a measurement cycle, the controlling computer code specified the probe current with an accuracy of 0.1 μA and provided simultaneous measurements of the probe voltage relative to the anode, the anode voltage, and the discharge current. The change in the probe current at each step was calculated automatically during the measurements with the help of a specially developed algorithm for optimizing the signal-to-noise ratio over the entire range of measured currents (a complete cycle of measurements of one *I–V* characteristic included from 1500 to 2000 steps). The measurements were carried out in the stroboscopic regime at a rate of 100 Hz synchronously with the oscillations of the supply voltage, thereby making it possible to avoid the influence of these oscillations on the experimental results. The gating time of the measured signals was 1 μs. The time delay (7 ms) of the measurement with respect to the beginning of the half-wave of the supply voltage was chosen so as to optimize the signal-to-noise ratio. After performing the measurements over the prescribed range of probe current variations, the measured data in the form of a dependence of the probe current on the probe potential for a given discharge current and given discharge voltage were stored as a computer file. With fixed experimental parameters, the *I–V* characteristic was measured up to 30 times. Thereafter, the data stored in the corresponding files were averaged over the measurement cycles.

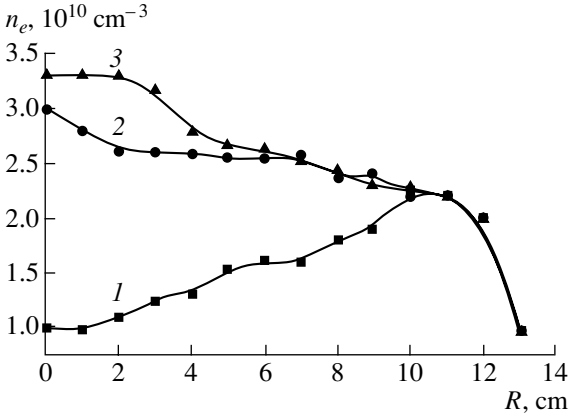

Fig. 1. Radial profiles of the electron density for different nitrogen pressures: (*1*) p = 0.1 torr, I_d = 0.63 A, and U_d = 470 V; (*2*) p = 0.06 torr, I_d = 0.73 A, and U_d = 580 V; and (*3*) p = 0.03 torr, I_d = 0.77 A, and U_d = 615 V.

The plasma potential was assumed to be equal to the probe potential at which the second derivative of the probe current with respect to the probe voltage vanishes. The plasma density was computed from the electron saturation current to the probe.

Figure 1 shows the radial profiles of the plasma density for different nitrogen pressures. We can see that the shape of the profiles is highly sensitive to the working gas pressure. For p = 0.1 torr, the plasma density is minimum at the cathode axis and increases gradually in the radial direction, reaching a maximum value at $R \approx$ 11 cm. At lower pressures (p = 0.03, 0.06 torr), the situation is radically different: the plasma density n_e is maximum at the axis of the system and decreases monotonically with radius. This dependence is peculiar to hollow-cathode discharges. At a pressure of 0.1 torr, essentially all of the energy of the fast primary electrons emitted from the cathode is expended on the excitation and ionization of the working gas within a distance of several centimeters from the cathode; consequently, the gas at the system axis is ionized mainly by the electrons that diffuse from the region where the plasma has already been produced. As a result, the plasma density is the highest not at the cathode axis but in the region where the loss of fast electrons is maximum and, accordingly, the plasma production is most intense. As the working gas pressure decreases, the maximum of the plasma density profile shifts toward smaller radii and, at $p \approx 0.05$ torr, it becomes bell-shaped.

Recall that, in gas discharges, a very important role is played by the electric field, which heats the plasma electrons and thus can substantially influence the shape

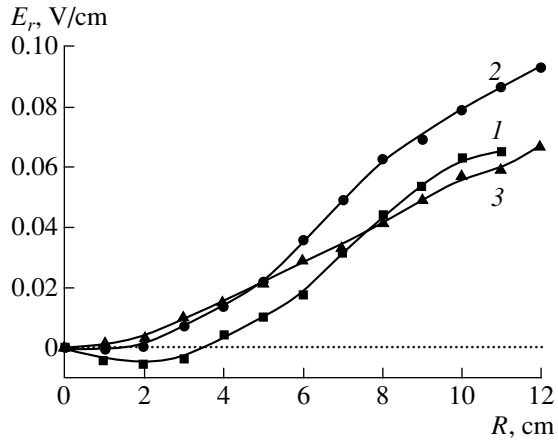

Fig. 2. Radial profiles of the radial electric field for different nitrogen pressures: (*1*) p = 0.1 torr, I_d = 0.63 A, and U_d = 470 V; (*2*) p = 0.06 torr, I_d = 0.73 A, and U_d = 580 V; and (*3*) p = 0.03 torr, I_d = 0.77 A, and U_d = 615 V.

of the EEDF. Figure 2 displays the experimentally measured radial profiles of the radial electric field E_r for different nitrogen pressures. The radial behavior of E_r is seen to be analogous to that of the plasma density. At low nitrogen pressures, the radial electric field is positive and increases monotonically with the radius. For p = 0.1 torr, the component E_r is negative in the axial region (where the plasma density is the lowest); at larger radii, it passes through zero and starts increasing monotonically. The maximum value of E_r does not exceed 0.1 V/cm. The longitudinal electric field E_z was found to be even weaker: the measurements showed that $E_z \approx 1\text{–}2 \times 10^{-2}$ V/cm for p = 0.1 torr, $E_z \approx 0.5\text{–}1 \times 10^{-2}$ V/cm for p = 0.06 torr, and $E_z < 10^{-2}$ V/cm for p = 0.03 torr. Below, we will show that such longitudinal and radial electric fields are too weak to significantly affect the shape of the EEDF.

The EEDF was measured at different points inside the vacuum chamber at different pressures of the working gas. Figures 3 and 4 show typical EEDFs measured at nitrogen pressures of 0.1 and 0.03 torr. We can see that the EEDF is strongly non-Maxwellian: it has a pronounced dip in the energy range 2–4 eV. Moreover, at a lower pressure (Fig. 3), there are two dips in the EEDF in this energy range.

We also established that, at low pressures, the EEDF is essentially independent of the radius, while, at p = 0.1 torr, the EEDF experiences fairly strong variations in the radial direction. Moreover, at the chamber axis (i.e., in the region where the reduced electric field E/N is minimum), the dip in the EEDF is the smallest. This radial behavior of the EEDF is not associated with the presence of an electric field, because the action of the electric field should result in the formation of an EEDF that depends on the radius in the opposite manner—the dip in the EEDF would be smallest at the discharge periphery, where the field is maximum. The observed reduction in the dip in the EEDF near the axis of a hollow cathode at high pressures (Fig. 4) may be attributed to the decrease in the number of high-energy electrons (which serve as the major energy source in the plasma) and, accordingly, to an increasingly important role of the processes that force the EEDF to evolve into a Maxwellian function. As was mentioned above (Fig. 1), it is precisely this pressure range in which the plasma density n_e is minimum at the chamber axis.

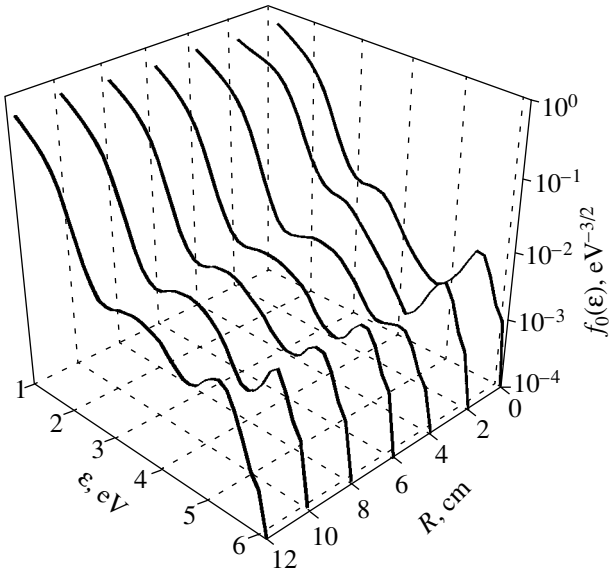

Fig. 3. EEDFs measured in nitrogen at a pressure of p = 0.03 torr at different radial positions R.

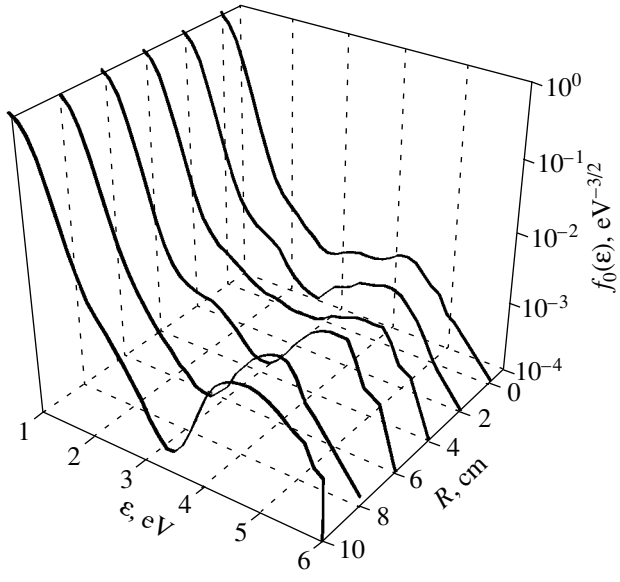

Fig. 4. EEDFs measured in nitrogen at a pressure of p = 0.1 torr at different radial positions R.

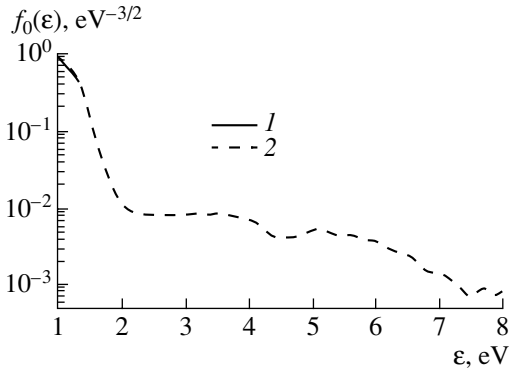

Fig. 5. EEDF measured in oxygen at a pressure of p = 0.06 torr at R = (*1*) 0 and (*2*) 9 cm.

The EEDF in an oxygen plasma is illustrated in Fig. 5, which shows that it is qualitatively different from the EEDF in N_2, although measurements were carried out in discharges with the same parameters. To a good accuracy, the EEDF in O_2 can be described by a Maxwellian function, but with different temperatures in the energy ranges ε = 0–2.5 eV and ε > 2.5 eV.

The physical reasons for such a large discrepancy between the EEDFs in N_2 and O_2 will be discussed in the next section.

3. THEORY

We calculated the EEDF by solving the Boltzmann equation in the two-term approximation [10]:

$$\frac{1}{n_e N}\left(\frac{m}{2e}\right)^{1/2}\varepsilon^{1/2}\frac{\partial(n_e f_0)}{\partial t} - \frac{1}{3}\left(\frac{E}{N}\right)^2\frac{\partial}{\partial\varepsilon}\left(\frac{\varepsilon}{Q_T}\frac{\partial f_0}{\partial\varepsilon}\right)$$
$$-\frac{\partial}{\partial\varepsilon}\left[2\frac{m}{M}Q_T\varepsilon^2\left(f_0 + T\frac{\partial f_0}{\partial\varepsilon}\right)\right] = S_{eN} + S_{ee} + A(\varepsilon), \quad (1)$$

where $f_0(\varepsilon)$ is the symmetric part of the EEDF; T is the gas temperature (in eV); $e = 1.602 \times 10^{-12}$ erg/eV; M is the mass of a molecule; N is the gas density; Q_T is the transport cross section; m is the mass of an electron; n_e is the electron density; S_{eN} is the integral of electron–neutral inelastic collisions; S_{ee} is the integral of electron–electron collisions; and $A(\varepsilon)$ is the ionization term, which includes the source of primary electrons. The expressions for the terms S_{eN}, S_{ee}, and $A(\varepsilon)$ were taken from [11].

Table 1

No.	Reaction	Threshold energy ε_{sh}, eV
1	$N_2 + e \longrightarrow N_2(v) + e$, $v = 1\ldots8$	1.5
2	$N_2 + e \longrightarrow N_2(A^3\Sigma_u^+) + e$	6.7
3	$N_2 + e \longrightarrow N_2(a^1\Pi_g) + e$	8.55
4	$N_2 + e \longrightarrow N_2(B^3\Pi_g) + e$	11.5
5	$N_2 + e \longrightarrow N_2^+ + e + e$	15.6
6	$N_2 + e \longrightarrow N + N + e$	9.76

The EEDF $f_0(\varepsilon)$ was normalized to satisfy the condition

$$\int_0^\infty \varepsilon^{1/2} f_0(\varepsilon)\,d\varepsilon = 1. \quad (2)$$

The electron processes that were taken into account when solving the Boltzmann equation for discharges in nitrogen and oxygen are listed in Tables 1 and 2. The superelastic scattering of electrons by vibrationally excited molecules was neglected, because, for the discharges under investigation, the specific input power and, accordingly, the vibrational temperature T_v were both much lower than those in the experiments of [4–8].

The cross sections for elastic and inelastic scattering of electrons by N_2 and O_2 molecules were taken from [12].

The calculations were carried out with the values of the electric field and electron density that were measured experimentally at different regions of the discharge chamber. The energy ε_n of the beam of primary electrons was assumed to be on the order of the potential drop across the cathode sheath, $\varepsilon_n \approx 400$ eV.

Equation (1) was solved using the same methods as in [10].

Figure 6 shows the EEDFs obtained theoretically for a hollow-cathode discharge in nitrogen. The EEDF was calculated for the parameter range (n_e, E) corresponding to the intervals of variation of n_e and E in the radial direction in the discharge chamber. For all values of the discharge parameters, there are two pronounced dips in the EEDF in the energy range ε = 2–4 eV. The dips are associated with the sharp peaks in the cross section for the vibrational excitation of N_2 molecules in this energy range. The EEDF calculated without allowance for the vibrational excitation of N_2 molecules is monotonic. Another factor that causes the dips in the EEDF to vanish is an artificial increase in E/N by an order of magnitude, up to the values that correspond to the experiments of [1–4] and are large enough for the EEDF to become Maxwellian.

Figure 7 shows the EEDFs calculated for an oxygen plasma. An important property in which oxygen differs from nitrogen is the presence of the metastable excited states of O_2 molecules, $O_2(^1\Delta_g)$ and $O_2(b^1\Sigma_g^+)$, with low threshold energies (0.95 and 1.64 eV, respectively). The EEDF calculated with allowance for the excitation of these states is cut off at energies of about 1–2 eV; this effect is especially pronounced for weak electric fields (Fig. 7). As for the processes of the vibrational excita-

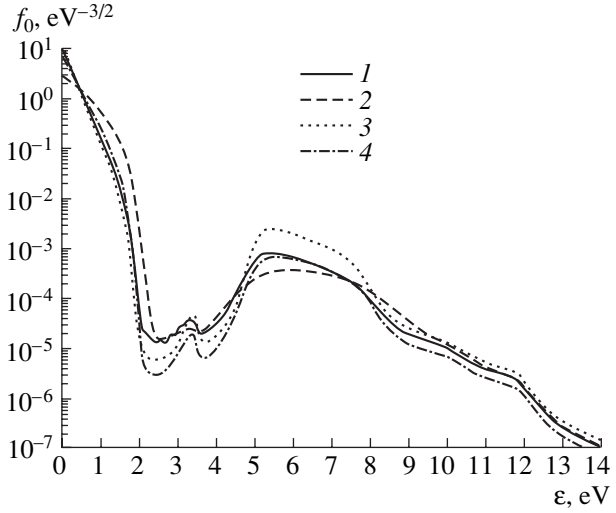

Fig. 6. EEDFs in nitrogen calculated for the parameter values (*1*) p = 0.03 torr, $n_e = 10^{10}$ cm^{-3}, and E = 0.01 V/cm; (*2*) p = 0.03 torr, $n_e = 10^{10}$ cm^{-3}, and E = 0.1 V/cm; (*3*) p = 0.1 torr, $n_e = 10^{10}$ cm^{-3}, and E = 0.01 V/cm; and (*4*) p = 0.1 torr, $n_e = 2 \times 10^{10}$ cm^{-3}, and E = 0.06 V/cm.

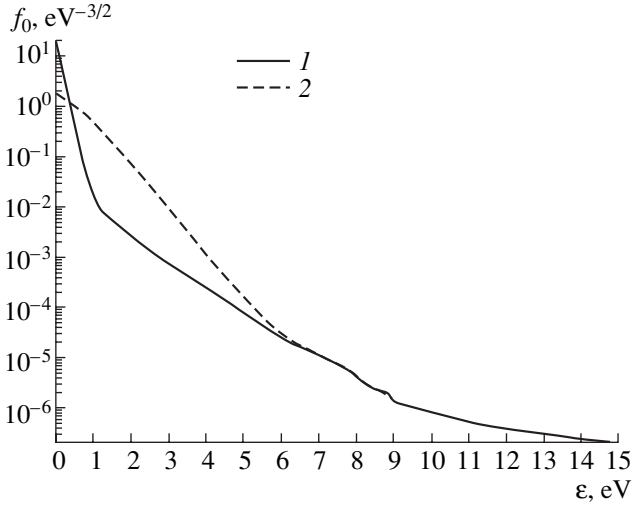

Fig. 7. EEDFs in oxygen calculated for p = 0.06 torr, $n_e = 10^{10}$ cm^{-3}, and E = (*1*) 0.01 and (*2*) 0.1 V/cm.

tion of O_2 molecules, they have essentially no influence on the EEDF because the vibrational excitation cross section for O_2 molecules is much smaller than that for N_2 molecules: up to the threshold energies for the excitation of electronic levels, the EEDF in an oxygen plasma can be described with good accuracy by a Maxwellian function with one or two (depending on the electric field magnitude) temperatures in different energy ranges.

4. DISCUSSION OF THE RESULTS

A comparison between the EEDFs measured experimentally in a nitrogen plasma at low pressures (Fig. 3) and the related EEDFs calculated theoretically (Fig. 6) shows that the experimental data agree well with theoretical predictions both qualitatively and quantitatively. In the energy range 2–4 eV, the positions of the measured and calculated dips in the EEDF coincide within an accuracy of 10–20%. In the measured EEDF, the dip that is closer to the right peak coincides with the relevant calculated dip within the limits of experimental error.

It should be noted that our experimental technique does not provide correct measurements of the EEDF in the energy range below 1 eV. Presumably, this is the reason why, in the range $\varepsilon < 1$ eV, the measured EEDF $f(\varepsilon)$ decreases to a lesser extent than the calculated EEDF. However, a comparison between the calculated and measured extents to which the EEDF decreases relative to its value at an energy of 1 eV also shows good agreement between theory and experiment.

At higher pressures, the agreement between the calculated and measured EEDFs is somewhat worse (Fig. 4), because, as was noted above, the radial energy distribution of the beam of fast electrons emitted by the cathode is highly nonuniform. In turn, the radial nonuniformity of the beam may be responsible for the nonlocal character of the EEDF, thereby giving rise to the loss of high-energy electrons at the axis of the discharge chamber. However, our calculations were carried out under the assumption that all of the parameters governing the EEDF are spatially uniform.

To within experimental error, the EEDF measured in an oxygen plasma (Fig. 5) also agrees well with the EEDF calculated for the electric field E = 0.01 V/cm with allowance for the above scattering cross sections (Fig. 7). Note that, in discharges in oxygen, the electric field was measured to be weaker than 0.02 V/cm. To a first approximation, the experimental EEDF can be described by two Maxwellian functions with different

Table 2

No.	Reaction	Threshold energy ε_{sh}, eV
1	$O_2 + e \longrightarrow O_2(v) + e$, $v = 1\ldots10$	1.95
2	$O_2 + e \longrightarrow O_2(^1\Delta_g) + e$	0.98
3	$O_2 + e \longrightarrow O_2(b^1\Sigma_g^+) + e$	1.64
4	$O_2 + e \longrightarrow O_2(A^3\Sigma_u^+) + e$	4.5
5	$O_2 + e \longrightarrow O_2(*) + e$	6.0
6	$O_2 + e \longrightarrow O_2(**) + e$	8.0
7	$O_2 + e \longrightarrow O_2(***) + e$	9.7
8	$O_2 + e \longrightarrow O_2^+ + e + e$	12.2
9	$O_2 + e \longrightarrow O + O + e$	6.0
10	$O_2 + e \longrightarrow O^- + O$	3.6

temperatures. Up to an energy of about 7 eV, the EEDF calculated theoretically for $E = 0.1$ V/cm is a one-temperature Maxwellian function; however, in our experiments with discharges in oxygen, such strong electric fields were not observed.

5. CONCLUSION

Hence, we have investigated the EEDF in hollow-cathode glow discharges in which the plasma is preferentially heated by fast electrons that are emitted from the cathode and are accelerated by the space charge electric field in the cathode sheath. We have revealed the following features of the EEDF:

(i) In discharges in nitrogen, there is a significant dip in the EEDF in the energy range $\varepsilon = 2$–4 eV. The dip is associated with the vibrational excitation of N_2 molecules.

(ii) In discharges in oxygen, the monotonic nature of the EEDF stems from the following two factors: first, the cross section for the vibrational excitation of oxygen molecules is smaller than that for nitrogen molecules and, second, the threshold energies for the excitation of the lowest lying metastable states of oxygen molecules are low.

The results of theoretical calculations agree well with the experimental data.

The measured and calculated EEDFs can be used to model the plasma kinetics and, accordingly, to determine the densities of all plasma components, thereby providing a good way to optimize the technologies based on hollow-cathode glow discharges. In addition, since the electric fields in such discharges are low, the EEDF adequately reflects inelastic electron processes and thus may give both qualitative and quantitative information about the cross sections for the corresponding processes in more complicated plasma-forming media.

REFERENCES

1. N. L. Aleksandrov, A. M. Konchakov, and É. E. Son, Fiz. Plazmy **4**, 169 (1978) [Sov. J. Plasma Phys. **4**, 98 (1978)].
2. V. Guerra and J. Loureiro, J. Phys. D **28**, 1903 (1995).
3. V. Guerra and J. Loureiro, Plasma Sources Sci. Technol. **6**, 373 (1997).
4. C. M. Ferriera and J. Lourero, Plasma Sources Sci. Technol. **9**, 528 (2000).
5. C. Gorse, M. Capitelli, and A. Ricard, J. Chem. Phys. **82**, 1900 (1985).
6. N. A. Gorbunov, N. B. Kolokolov, and A. A. Kudryavtsev, Zh. Tekh. Fiz. **58**, 1817 (1988) [Sov. Phys. Tech. Phys. **33**, 1104 (1988)].
7. N. A. Gorbunov, N. B. Kolokolov, and A. A. Kudryavtsev, Zh. Tekh. Fiz. **61** (6), 52 (1991) [Sov. Phys. Tech. Phys. **36**, 616 (1991)].
8. N. A. Oyatko, Yu. Z. Ionikh, N. B. Kolokov, *et al.*, J. Phys. D **33**, 2010 (2000).
9. Yu. A. Ivanov, Yu. A. Lebedev, and L. S. Polak, *Contact Diagnostics in Nonequilibrium Plasmochemistry* (Nauka, Moscow, 1981).
10. A. I. Shchedrin, A. V. Ryabtsev, and D. Lo, J. Phys. B **29**, 915 (1996).
11. J. P. Shkarofsky, T. W. Johnston, and M. P. Bachynski, *The Particle Kinetics of Plasmas* (Addison-Wesley, Reading, 1966; Atomizdat, Moscow, 1969).
12. I. A. Soloshenko, V. V. Tsiolko, V. A. Khomich, *et al.*, Fiz. Plazmy **26**, 845 (2000) [Plasma Phys. Rep. **26**, 792 (2000)].

Translated by I. A. Kalabalyk